Optically inspired biomechanical model of the human eyeball

Wieslaw Śródka
Wroclaw University of Technology
Faculty Division of Deformable Body Mechanics
Poland

D. Robert Iskander
Queensland University of Technology
School of Optometry
Australia

Abstract. Currently available biomechanical models of the human eyeball focus mainly on the geometries and material properties of its components while little attention has been given to its optics—the eye's primary function. We postulate that in the evolution process, the mechanical structure of the eyeball has been influenced by its optical functions. We develop a numerical finite element analysis-based model in which the eyeball geometry and its material properties are linked to the optical functions of the eye. This is achieved by controlling in the model all essential optical functions while still choosing material properties from a range of clinically available data. In particular, it is assumed that in a certain range of intraocular pressures, the eye is able to maintain focus. This so-called property of optical self-adjustments provides a more constrained set of numerical solutions in which the number of free model parameters significantly decreases, leading to models that are more robust. Further, we investigate two specific cases of a model that satisfies optical self-adjustment: (1) a full model in which the cornea is flexibly attached to sclera at the limbus, and (2) a fixed cornea model in which the cornea is not allowed to move at the limbus. We conclude that for a biomechanical model of the eyeball to mimic the optical function of a real eye, it is crucial that the cornea is allowed to move at the limbal junction, that the materials used for the cornea and sclera are strongly nonlinear, and that their moduli of elasticity remain in a very close relationship.
[DOI: 10.1117/1.2952189]

Keywords: human eye; opto-mechanical properties; finite element analysis.

Paper 07387RR received Sep. 19, 2007; revised manuscript received Feb. 6, 2008; accepted for publication Feb. 8, 2008; published online Jul. 10, 2008.

1 Introduction

It is much easier to construct a numerical model of the human eyeball nowadays than it was 20 to 30 years ago due to advances in professional software programs for construction design based on finite element analysis (FEA). Such programs allow the construction of models of a complete eye globe with complicated geometry that possess both nonlinear and anisotropic materials.[1,2] However, most of the work done with such numerical tools has been dedicated to the specific elements of the eye globe, and in particular to the cornea and its mechanical properties, before and after corneal refractive surgery.[3–5] Also, there has been a continuous effort to model and analytically describe the mechanical properties of the eye using closed-form expressions.[6,7]

Thus, it would appear that biomechanical modeling of the eyeball should have been resolved and that the accuracy of such a model would only be a matter of performing a larger number of iterations to find the numerical solution. However, notwithstanding the efforts that are being made toward development of accurate algorithms, current eye models are still far from describing the behavior of a real human eye. The reason for this is rather prosaic. Despite the eye's apparent structural simplicity, the *in vivo* mechanical properties of the human eye have not been categorically described. Using the words of Shin et al.[8] in referring to the cornea, "experimental data is [often] meagre and flawed." Detailed knowledge of the structure of all eyeball tissue components (i.e., cornea, sclera, iris, lens, choroid, and retina) as well as their material properties (nonlinear and anisotropic) is needed. Two of these eyeball components, the cornea and the sclera, are fairly well described when it comes to their geometries, but their material properties have been disputed.[8–14] On the other hand, knowledge of the *in vivo* mechanical properties of the other components of the eye is very limited. As a result, most reported biomechanical models of the human eyeball contain the cornea and the sclera, and sometimes the optic nerve,[15] but omit the other components.

Another deficiency in the majority of reported biomechanical models of the eyeball is the developers' apparent low interest in the optics of the eye. Most authors develop their models as if the eye was a strictly mechanical structure while

Address all correspondence to: D. Robert Iskander, School of Optometry, Queensland University of Technology, Victoria Park Road, Kelvin Grove, Brisbane, Queensland 4059, Australia. Tel: 61 7 31385705; Fax: 61 7 31385665; E-mail: d.iskander@qut.edu.au

1083-3668/2008/13(4)/044034/8/$25.00 © 2008 SPIE

its optics was just a simple consequence of the mechanical parameters, which are often chosen *ad hoc*. Subsequently, this often leads to problems with accurate mechanical identification. To date, optical properties of the eye are hardly used to identify the mechanical parameters of the eyeball model.[16]

In this work we postulate that the optical functions of the eye have strongly influenced its mechanical structure; that it is the optics of the eyeball that took, in the evolution process, control over the mechanics (in terms of geometry and material parameters) and subjected it toward its needs.[17] It is well known from studies on a variety of species that there is a direct role of vision in the material properties of the eye and in regulation of its growth.[18,19] Therefore, it is highly likely that the material properties of the eye must have been selected by nature to optimize the optics and visual function in the first place. Thus, biomechanical modeling of the eyeball should include some relationships between the mechanical and optical parameters of the eye so the goal of developing an accurate mechanical eyeball model can be achieved.

Using this concept, we develop a numerical model of an eyeball in which the structural parameters (in terms of the eyeball geometry and its material properties) are linked to the optical function of the eye. This is achieved by controlling in the model all essential optical functions of the eye while still assuming material properties from the range of those available in the literature experimental results.[20–23] By combining the mechanical and optical functions of the eye in the model, the number of free model parameters significantly decreases, which makes the model more robust and the comparison between any two model conditions more tractable.

2 Methods

A model of the eyeball is defined as a set of geometrical and material parameters in the design of a mechanical construction that can be solved using the finite element method (FEM). In this view, the type of the elements used or the particular solution parameters of the FEM is of some importance, as they may have a significant impact on the accuracy of the solution.

2.1 *The FEM Model*

The model that we use to link the mechanical properties of the eye to its optical functions is built from a 2-D quadrilateral 8-node body of revolution elements. More than 500 of such elements were used. The solution parameters include both the nonlinear material effects as well as the changes in the construction configuration under loading.

A typical distribution of the density of elements used in our model is shown in Fig. 1. The boundary conditions (model mounting) limit the movements of the construction as a rigid body; otherwise the model is allowed to move freely. The model includes three kinds of material properties corresponding to the cornea, sclera, and limbus (the circled area in Fig. 1). The only material that can remain linear in a model and satisfy optical self-adjustment is that of the limbus. Its Young's modulus is set to $E=1$ MPa. All numerical calculations have been performed using Cosmos/M™.[24]

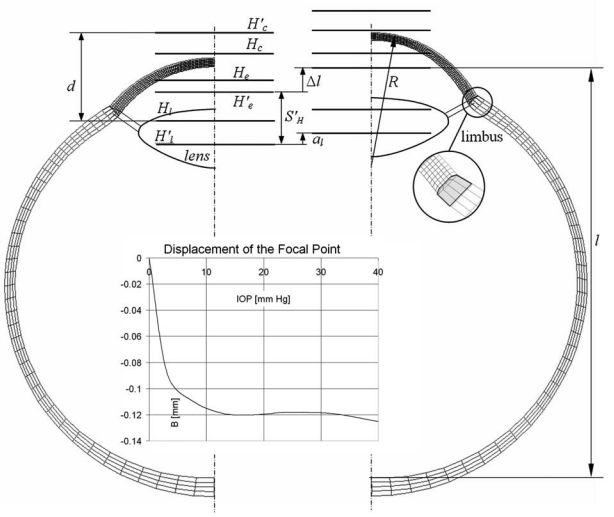

Fig. 1 Geometry of the eyeball model used for the FEM together with the displacements of the main optical plains for the cornea and the crystalline lens caused by the increase in IOP. The inset shows the displacement of the focal point which, in the range between 12 and 38 mm Hg, does not significantly change, making the model optically self-adjusted.

2.2 *Assumption of Optical Self-Adjustment*

The phenomenon of optical self-adjustment of the eye can be observed during an increase in intraocular pressure (IOP). One would expect that an increase in IOP could result in a slight expansion of the eyeball and the following sequence of actions:

1. Corneal apex moving away from the retina,
2. Slight change in corneal curvature,
3. Slight axial movement of the limbus (that is internally attached to crystalline lens), and
4. Increase in the axial distance between the cornea and the crystalline lens (see parameter d in Fig. 1).

Such deformations would influence the position of the focal point of the eye's optical system (here we do not consider the accommodative properties of the crystalline lens). However, it appears that it is possible to "tune" the geometries and material properties of the cornea, limbus, and sclera in such a way so that the focal point would remain in place in a given range of IOP values. Thus, the self adjustment is understood as the result of a subtle arrangement of eyeball mechanical parameters to ensure that the retinal image remains stable in the presence of fluctuations in IOP. Figure 1 illustrates this mechanism. It should be noted that optical self-adjustment is related to the mechano-optical response of the eye to changes in IOP. This response is almost instantaneous, so there is no time for the eye to respond in a rheological deformation or to accommodate. This hypothesis was postulated earlier,[17] and we used it in our earlier work where a solution for a linear model of the eyeball was devised.[16] Recent clinical studies of McMonnies and Boneham provide further support for the postulate, though it has not been proved.[25,26] Under the assumptions given in the postulate, our preliminary study indicated that the following structural parameters of the eyeball have the largest impact on the property of self adjustment:

Table 1 Main parameters of the considered model of the eyeball.

Parameter	Source (e.g.)	Value
Central anterior radius of curvature	Kiely et al.[28]	$R=7.84$ mm
Central posterior radius of curvature	Edmund[20]	$r=6.75$ mm
Central corneal thickness	Liu et al.[22]	CCT=0.52 mm
Peripheral corneal thickness adjacent to the limbus	Dubbelman et al.[29]	PCT=0.65 mm
Diameter of the cornea	Baumeister et al.[30]	$D_c=11.5$ mm
Average corneal refractive index	Patel et al.[21]	$n_c=1.3771$
Average refractive index of aqueous humour and vitreous body	Le Grand and El Hage[27]	$n_a=1.336$
Refractive power of the crystalline lens	Le Grand and El Hage[27]	$F_{lens}=22.07$ D
Poisson ratio	(see text)	$\nu=0.49$
Nominal intraocular pressure	Eysteinsson et al.[23]	IOP=16 mm Hg

1. The ratio of the corneal longitudinal modulus of elasticity to that of the sclera,
2. Limbus ring stiffness, and
3. The geometry of the anterior surface of the cornea.

2.3 *Model Geometry*

We approximate the anterior and posterior surfaces of the cornea by spheres similar to the Gullstrand—Le Grand model,[27] making sure that the data follow the available knowledge based on experimental measurements. The nominal parameter values for the considered eyeball are shown in Table 1 for a model under no load. Changes of these parameters with the increasing level of IOP will be shown later. The sclera is modeled as a 12.5-mm anterior radius sphere with varying thicknesses: 0.8 mm near the limbus, 0.6 mm in the equatorial area, and about 1 mm in the foveal region (see Fig. 1).

The corneal surfaces are better modeled by aspheric surfaces, such as an ellipsoid,[31,32] because those shapes correspond better to keratometric measurements of real corneas than a sphere. In our previous study on optical self-adjustment,[16] we did consider an elliptic shape with eccentricity $e=0.5$. This result, however, was achieved for a linear model. Here, we decided to use the classical spherical model of the cornea so we could first study the behavior of a model with nonlinear materials.

2.4 *Boundary Conditions*

There is no agreement in the literature on how the model of the eyeball should be mounted despite the fact that there are many studies devoted to orbital mechanics of the eye.[33–36] For obvious reasons, those analytical models that consider the corneal surface only have either a roller or a fixed support.[12–14] However, such simplified mountings are also considered in numerical models.[3,8,37] As we will show later, this could lead to misinterpretation of the numerical results, particularly when dealing with the optical function of the eye. A recent *in vivo* study on corneal rigidity[38] supports the assumption of free mounting the eyeball, which we will also adopt here.

2.5 *Materials*

The anterior surfaces of cornea and sclera have been well documented and their physical structures are known.[39] However, the knowledge of their mechanical properties is less complete. It is known that the materials are nonlinear, anisotropic, and that under a large load, their rheological properties must be taken into account. Fortunately, not all of these aspects need always to be considered. In particular, for a model of a normal living eye, one can assume an isotropic and elastic material. However, this material must be *nonlinear*. Here we also restrict ourselves to only one layer of corneal tissue, and from this point onward we identify the cornea with the stroma. This simplification does not significantly reduce the accuracy of the solution,[2] since it appears that the Young's modulus of the Descemet's membrane is much smaller than that of the stroma.[40]

The stress-strain functional relationship, $\sigma=f(\varepsilon)$, that can be used to characterize the eye surface materials can be expressed in the known exponential form[39,41]

$$\sigma = A[\exp(\alpha\varepsilon) - 1], \quad \varepsilon \geqslant 0, \tag{1}$$

where A and α are constants related to material properties. This functional relationship has an important property that its derivative, known as the tangential modulus of elasticity, is nonzero for strain values approaching zero, i.e.,

$$E_0 = \left.\frac{d\sigma}{d\varepsilon}\right|_{\varepsilon\to 0} = A\alpha. \tag{2}$$

For the negative stress, we will assume that the material properties are governed by a linear relationship:

$$\sigma = E_0\varepsilon, \quad \varepsilon < 0. \tag{3}$$

The anisotropy of the secant modulus of elasticity, dependent on the sign of the strain, is associated with the molecular structures of the stroma and sclera.[39] The constitutive Eqs. (1) and (3) approximate mechanical functions of a real human cornea, particularly in a clinically relevant range of IOP. The secant modulus of elasticity is often expressed in a form $E_{\text{Secant}}=\sigma/\varepsilon$. In our case, the secant modulus of elasticity is given by

$$E_{\text{Secant}} = \frac{A[\exp(\alpha\varepsilon) - 1]}{\varepsilon}. \tag{4}$$

Despite the fact that expression (4) is a function, we will still call it a modulus. It should, however, be distinguished from

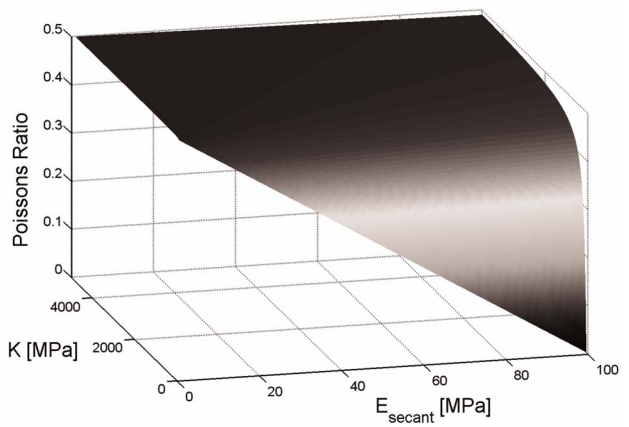

Fig. 2 Poisson's ratio as a function of bulk modulus and secant modulus.

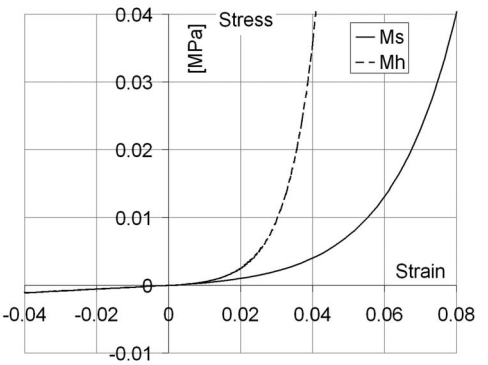

Fig. 3 Stress-strain relationship for the two considered nonlinear materials.

the Young's modulus, which is constant and used for linear materials only.

In the analysis of the stress state present in ocular surfaces under IOP, we also need to consider the value of another variable: the Poisson's ratio. The limit of the Poisson's ratio for an isotropic incompressible material (e.g., water) is $\nu=0.5$, and in some works it has been used to describe corneal tissue.[3,42] However, this limit value cannot be used in our modeling, because the stress-strain relationship in this case is no longer uniquely described. For this reason, we consider Poisson's ratio values of the eye constructions values that are just below this limit. The problem is that Poisson's ratios ranging from $\nu=0.15$ through $\nu=0.3$ to $\nu=0.49$ are being reported.[2,8,37,43,44] However, this wide range of values is being disputed, because some of the considered values are supported by real measurements.[1,45] In some cases, the use of real measurements and the belief that they are correct may lead to an unrealistic situation. See, for example, the work of Pandolfi and Manganiello,[37] where the chosen values of the secant modulus of elasticity and the Poisson's ratio led to unrealistically low values of the bulk modulus. In our opinion, such a discussion is of no serious significance because the model solution only marginally depends on the Poisson's ratio. If we assume that the bulk modulus of elasticity of considered soft tissues is of the same order as that of water ($K=2200$ MPa), that is 10^3 MPa, while their secant (Young's) modulus of elasticity is about three orders smaller, i.e., 10^0 MPa, then the Poisson's ratio is

$$\nu = \frac{3K - E}{6K} = \frac{3000 - 1}{6000} = 0.4998.$$

It is worth noting that varying the parameters K and E within the range of values that can be attributed to ocular tissues does not change this ratio significantly (see the mostly flat region of the relationship in Fig. 2). For this reason, we will assume in our modeling the value of $\nu=0.49$.

The material parameters of the considered biomechanical model of the eyeball have been chosen in a way so that the model results match those of the Goldmann applanation tonometry.[46] Despite its deficiencies it is still the most widely accepted method of determining intraocular pressure.[47,48] In this technique, the cornea is modeled as a membrane filled with fluid under certain pressure. Then, using a specially calibrated probe, a small force is applied to the central 3.06-mm-diameter flattened corneal area, which in turn exerts a force directly related to the internal pressure as per the so-called Imbert-Fick law.

Identification of the corneal material parameters with the Goldmann's test showed that, to adequately represent the performance of a real eye in our modeling, the following criteria must be met:

1. The material [function $\sigma=f(\varepsilon)$] must be strongly nonlinear (even under the physiological load).
2. The modulus E_0 from Eq. (2) must be relatively small (of an order of magnitude smaller than the average secant modulus of the cornea, E_{Secant}, for IOP $=16$ mm Hg.
3. The material elasticity E_{Secant} for $\varepsilon<0$ must be much smaller than that for stretching, as described in Eq. (3).

Using all the above information and criteria, we set two extreme limit materials for the material properties of the cornea for which the biomechanical model would behave close to the performance of a real eye observed clinically. The most pliable material (the softest), denoted by M_s, and the stiffest (the hardest), denoted by M_h, had the following parameters:

$$M_s\text{: } A = 500 \text{ Pa}, \quad \alpha = 55, \quad \text{for } \varepsilon \geqslant 0, \quad \text{and } E_0 = 0.0275 \text{ MPa for } \varepsilon < 0; \tag{5}$$

$$M_h\text{: } A = 200 \text{ Pa}, \quad \alpha = 130, \quad \text{for } \varepsilon \geqslant 0, \quad \text{and } E_0 = 0.0260 \text{ MPa for } \varepsilon < 0. \tag{6}$$

Note that for a given stress value, the strain in material M_s was about twice that encountered in material M_h. Figure 3 shows the stress-strain relationships for the two considered materials.

The assumption that the model satisfies the principle of optical self-adjustment leads to another structural condition. Specifically, for a given stress value, the secant modulus of the sclera must be several times larger than that of the cornea. By denoting this relationship by

$$m = \frac{E_{\text{Secant}}(\text{sclera})}{E_{\text{Secant}}(\text{cornea})}, \tag{7}$$

it follows that the material used for the sclera is given by the following stress-strain function:

$$\sigma = A[\exp(m\alpha\varepsilon) - 1], \quad \varepsilon \geqslant 0, \tag{8}$$

where the constant A is the same as the one used for the cornea. We have determined ratio m in our preliminary studies to be in the range between 4.6 and 6. This ratio has its significance even in a linear model of the eyeball[49] and has its confirmation in experimental studies.[9]

We have numerically validated this proposed nonlinear model by comparing its stiffness to that of a real eye.[38,50] In this particular aspect, material M_h showed much better performance than that given by material M_s. That is why in the remaining part of this paper we will only consider the corneal model realized from material M_h. The material for the sclera, on the other hand, satisfies relationship (8) with $m=5$.

Finally, the main role of the limbus in the model is to "optically couple" the cornea and sclera so that optical self-adjustment is satisfied. The limbus is defined as an annular transition zone between the cornea and sclera. Histologically, at the limbus, the epithelium gradually thickens toward the sclera where it is replaced by conjunctival tissue. In our modeling, we simplify this limbus area to a limbus ring with mechanical properties that are between those of the cornea and sclera. Since the secant modulus of the cornea is close to 0.5 MPa and that of the sclera is $m=5$ times larger, i.e. 2.5 MPa, the modulus for the limbus must be set between these two values, say $E=1$ MPa, so that the structure is not perturbed.

2.6 *Optical System of the Eyeball*

The total optical power of the eye depends on the respective powers of the cornea and crystalline lens and their mutual positions (i.e., distance d). Figure 1 shows the optical system and the notation used. The parameters of the eyeball are given in Table 1. Changes in the pressure p influence the optical power of the cornea (by changing its axial curvature R) as well as the distance d between the cornea and the crystalline lens.

The optical power of the eyeball is given by.

$$F_{\text{eye}} = F_{\text{cornea}} + F_{\text{lens}} - \frac{d \cdot F_{\text{cornea}} \cdot F_{\text{lens}}}{n}, \tag{9}$$

while its focal length is

$$f = \frac{n}{F_{\text{eye}}}. \tag{10}$$

Here it is assumed that the power of the lens F_{lens} is constant, but the distance d and the power of the cornea,

$$F_{\text{cornea}} = \frac{n-1}{R}, \tag{11}$$

depend on the pressure p. Both d and R are obtained from the FEM solution. The above formula describes the optical power of the anterior corneal surface that divides areas of significantly different refractive indices (i.e, $n=1$ for air, and $n_c = 1.3771$ for the cornea). The contribution of the posterior corneal surface to total power changes is just above 1%. However, this contribution is much lower when changes in optical power are considered. That is why we remain with formula (11) in all further calculations.

The displacement of the focal point with respect to the back of the eye is influenced not only by the changes in optical power of the cornea-crystalline-lens interface, but also by the "optical" elongation of the eyeball, which is understood here as a shift of the secondary principal plane H'_e with respect to the back of the eye. Thus, displacement of the focal point is composed of the axial elongation of the sclera (i.e., axial translation of the crystalline lens a_l) and the change in the distance S'_H between the crystalline lens and the second principal plane H'_e (see Fig. 1),

$$\Delta l = a_l + \Delta S'_H. \tag{12}$$

The distance S'_H is given by

$$S'_H = d \cdot F_{\text{cornea}}/F_{\text{eye}},$$

while the axial translation of the crystalline lens a_l is obtained from the FEM solution.

Finally, the displacement in focus (positive sign toward the cornea) is given by

$$B = \Delta l - \Delta f. \tag{13}$$

The function B can be treated as a measure of optical blur on the retina. If its change is due to the intraocular pressure p, then the criterion of optical self-adjustment can be analytically expressed as

$$\frac{dB}{dp} = 0. \tag{14}$$

The deformation of the sclera has a crucial role in the above criterion. Thus, studying optical self-adjustment in models that contain only the corneal surface that is fixed at its perimeter is an oversimplification.

The property of optical self-adjustment determines the ratio of the corneal longitudinal modulus of elasticity to that of the sclera (parameter m). Together with the material properties of the cornea, they "automatically" determine the parameters of the sclera and limbus, hence reducing the number of free parameters used in the model.

3 Results

3.1 *Full Model*

First, we consider a full model of the eyeball with standard geometry (see Table 1), material M_h, and free movement mounting under internal load p. The free model parameters include the thickness of the sclera (0.8 mm near the limbus, 0.6 mm in the equatorial area, and about 1 mm in the foveal region), the central corneal thickness (CCT), peripheral corneal thickness adjacent to the limbus (PCT), central anterior radius of curvature, parameters A and α of the corneal material, and the ratio m.

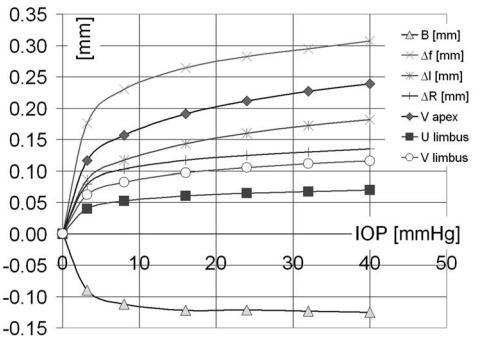

Fig. 4 Parameters of the full model as functions of intraocular pressure p. B is the displacement in the focus, Δf is the displacement in the focal point with respect to H'_e, Δl is the change in eye length, ΔR is the change in the central anterior corneal radius of curvature, V_{Apex} is the axial displacement of the corneal apex, and V_{Limbus} and U_{Limbus} are the axial and radial displacements of the limbus.

Figure 4 shows the solutions of the FEM for several functions dependent on p. The load was applied in steps and the FEM solutions were fast-converging. The solutions include B, the displacement in the focus; R, the central anterior corneal radius of curvature; V_{Limbus} and U_{Limbus}, the axial and radial displacements of the limbus; and V_{Apex}, the axial displacement of the corneal apex. Comparing the displacement in the focus $B(p)$ with the displacements in the corneal curvature and limbus, we note that they are all of the same order, say about 0.1 mm. However, function $B(p)$ shows that for the pressure larger than 10 mm Hg, the changes in displacement of focus are much smaller; thus, the model fullfills the criterion of optical self-adjustment. Note also that because the cornea has a flexible mount at the limbus, its radius of curvature R increases with the pressure p.

Figure 5 shows the radial profile of the anterior cornel surface for the same seven loads considered in Fig. 4, i.e., from 0 mm Hg to 40 mm Hg in steps of 8 mm Hg, and additionally for $p=3.2$ mm Hg, for which the displacements are most rapid.

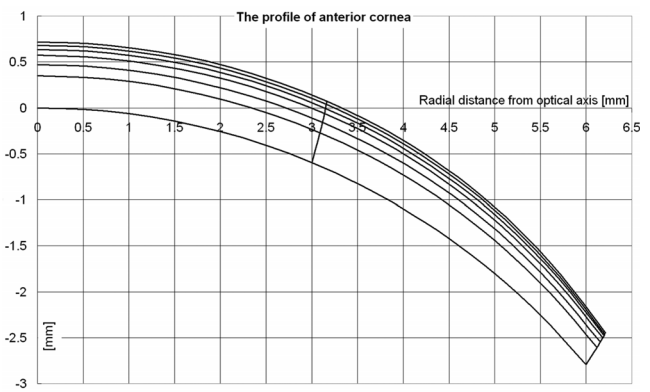

Fig. 5 Radial profile of the anterior corneal surface (the displacements are magnified 3×) for the same seven loads considered in Fig. 3, i.e., from 0 to 40 mm Hg in steps of 8 mm Hg, and additionally for $p=3.2$ mm Hg. The average angle of trajectory of the limbus is 58 deg. The limbal ring limits the movements of the limbus, causing a larger displacement of the corneal apex.

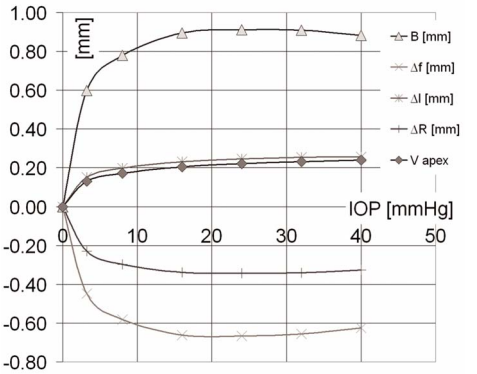

Fig. 6 Parameters of the fixed cornea model as functions of intraocular pressure p. B is the displacement in the focus, Δf is the displacement in the focal point with respect to H'_e, Δl is the change in eye length, ΔR is the change in the central anterior corneal radius of curvature, and V_{Apex} is the axial displacement of the corneal apex.

3.2 *Fixed Cornea Model*

In many applications, it is a quite common practice to reduce the full model of the eyeball to a model of the cornea that is fixed at the limbus.[5,13,47] However, such an approach significantly alters the results of the calculated optical power of the model because it significantly changes the location of the focal point with respect to the cornea. It also changes other optical functions of the eye that are important in biomechanical studies of the eyeball.

The FEA solution for the fixed cornea model is similar to that of a model with a limbal ring that has infinitely high stiffness. However, two such models are not identical, because in the fixed corneal model the sclera expands. Figure 6 indicates that the optical mechanism of this model is different than that of the full model described earlier (see Fig. 4). The most important difference is in the shape of function ΔR. That is, unlike in the full model, the central anterior corneal radius of curvature decreases with an increase in p. As a consequence, the focal distance in the fixed cornea model shortens and its amplitude gets larger than in the case of the full model. Also, the displacement of the focal point differs with changes in p—it moves forward much more while previously it moved slightly backward. The reason for all of these differences between the two considered models is the dynamic behavior of the anterior corneal surface when it is fixed at the limbus (see Fig. 7). However, it is counterintuitive that these radically different boundary conditions lead also to a model that is optically self-adjusted in the range from 16 mm Hg to 32 mm Hg [see function $B(p)$ in Fig. 6]. It should be noted that it is not easy to achieve optical self-adjustment for the model. For the material M_h, a deviation from criterion (7) and $E_{\text{Limbus}}=1$ MPa quickly puts the model "out of tune" in which function $B(p)$ changes strongly in the whole range of considered pressures.

4 Discussion

We have considered biomechanical models of a standard eyeball (surgically unaltered). The FEA solutions of the two considered models clearly indicate that the boundary conditions (in particular the way the cornea is fixed to the sclera)

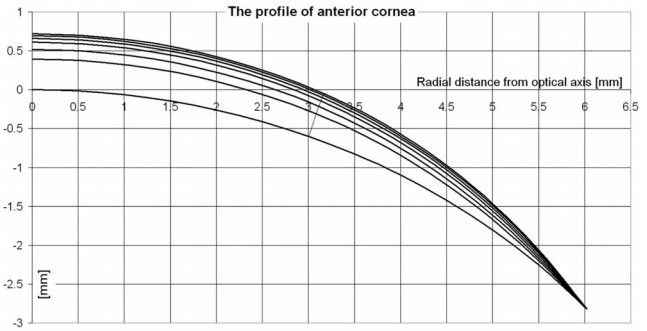

Fig. 7 Radial profile of the anterior cornel surface (the displacements are magnified 3×) for the same seven loads considered in Fig. 5. Unlike in the full model, here the limbus is fixed and not allowed to move.

strongly influence the optics of the eyeball. The investigated case of the fixed cornea model is somewhat extreme. However, even for the model with the roller support of the cornea[3,13] at 40 to 45 deg, it is not possible to achieve optical self-adjustment because this type of support does not fullfill condition (7).

Thus, the most important feature of our proposed optically inspired model is its optical self-adjustment for intraocular pressure above 10 mm Hg. The principal condition for such behavior of the eye model is the constraint on the secant modulus of the sclera to be several times larger than that of the cornea. The Young's modulus of the limbal ring, $E_{\text{Limbus}}=1$ MPa, also had to be chosen carefully. It is quite remarkable that these purely mechanical conditions were imposed simply by the optics.

These modeling results have indicated that the increase of focal length Δf, as well as the corresponding change in eye length Δl, are functions of p and are closely related for pressures above 10 mm Hg since their difference (equal to B) is almost constant. For example, for $p=16$ mm Hg, the focal length changed by $\Delta f=0.264$ mm (from the clinically unseen in a real eye but biomechanically relevant case where $p=0$). If the length of the eye had not changed at the same time, one would expect that the focal point had moved by this value. However, in the optical self-adjustment model, the focus moved only by about $B=-0.121$ mm, a difference of about 0.7 to 0.3 D (again, from the nominal point of $p=0$). Note that in a real eye, where the intraocular pressure may range between 10 and 20 mm Hg, the condition of optical self-adjustment results in changes of focal point that are not noticeable by a human.

The solutions for the fixed cornea model (shown in Figs. 6 and 7 indicate that it is a drastically different model. The displacement of the second principal plane Δl, despite originating mainly from the displacement of the crystalline lens $\Delta S'_H$ [see Eq. (12)], is much larger than in the full model. However, the largest difference can be seen in changes of the focal point Δf with respect to the initial value of $f=22.426$ (for $p=0$). Not only has the change radically increased, but the sign also changed. Instead of moving by −0.121 mm (backward), it moved by 0.894 mm (forward). This leads to significant optical power changes:

$$\Delta F_{\text{eye}} = \frac{1.336}{0.022426 - 0{,}000894} - \frac{1.336}{0.022426 + 0.000121}$$
$$= 62.05 - 59.25 = 2.8\text{D}.$$

Thus, fixing the limbus results in a completely different optical model of the eyeball than in the case where the cornea is attached to the flexible sclera.

The displacements of the limbus, although small, have a crucial impact on the optical power F_{eye} of the whole system being a function of the intraocular pressure p. This functional relationship has an important role in the numerical studies of the eyeball. On the other hand, the displacements of the limbus caused by changes in p depend on the material properties of both the sclera and the limbal ring. Therefore, it is important that these displacements are carefully considered in numerical models of the eyeball.

Acknowledgments

The authors wish to thank Henryk Kasprzak for his encouragement, comments, and helpful suggestions. Part of this research was supported by the Australian Research Council 2007 Linkage Grant, LX0775988.

References

1. E. Uchio, S. Ohno, J. Kudoh, K. Aoki, and L. T. Kisielewicz, "Simulation model of an eyeball based on finite element analysis on a supercomputer," *Br. J. Ophthamol.* **83**, 1106–1111 (1999).
2. H.-L. Yeh, T. Huang, and R. A. Schachar, "A closed shell structured eyeball model with application to radial keratotomy," *J. Biomech. Eng.* **122**(5), 504–510 (2000).
3. K. Anderson, A. El-Sheikh, and T. Newson, "Application of structural analysis to the mechanical behaviour of the cornea," *J. R. Soc., Interface* **1**(1), 3–15 (2004).
4. D. Cabrera Fernández, A. M. Niazy, R. M. Kurtz, G. P. Djotyan, and T. Juhasz, "Finite element analysis applied to cornea reshaping," *J. Biomed. Opt.* **10**(6), 064018 (2005).
5. V. Alastrué, B. Calvo, E. Peña, and M. Doblaré, "Biomechanical modeling of refractive corneal surgery," *J. Biomech. Eng.* **128**(1), 150–160 (2006).
6. P. R. Greene, "Closed-form ametropic pressure-volume and ocular rigidity solutions," *Am. J. Optom. Physiol. Opt.* **62**(12), 870–878 (1985).
7. P. M. Pinsky, D. van der Heide, and D. Chernyak, "Computational modeling of mechanical anisotropy in the cornea and sclera," *J. Cataract Refractive Surg.* **31**(1), 136–145 (2005).
8. T. J. Shin, R. P. Vito, L. W. Johnson, and B. E. McCarey, "The distribution of strain in the human cornea," *J. Biomech.* **30**(5), 497–503 (1997).
9. S. L.-Y. Woo, A. S. Kobayashi, W. A. Schlegel, and C. Lawrence, "Nonlinear material properties of intact cornea and sclera," *Exp. Eye Res.* **14**(1), 29–39 (1972).
10. E. Sjøntoft and C. Edmund, "*In vivo* determination of Young's modulus for the human cornea," *Bull. Math. Biol.* **49**(2), 217–232 (1987).
11. T. R. Friberg and J. W. Lace, "A comparison of the elastic properties of human choroid and sclera," *Exp. Eye Res.* **47**, 429–436 (1988).
12. J. Ø. Hjortdal, "Regional elastic performance of the human cornea," *J. Biomech.* **29**(7), 931–942 (1996).
13. G. J. Orssengo and D. C. Pye, "Determination of the true intraocular pressure and modulus of elasticity of the human cornea," *Bull. Math. Biol.* **61**(3), 551–572 (1999).
14. C. Boote, S. Dennis, R. H. Newton, H. Puri, and K. M. Meek, "Collagen fibrils appear more closely packed in the prepupillary cornea: optical and biomechanical implications," *Invest. Ophthalmol. Visual Sci.* **44**(7), 2941–2948 (2003).
15. A. J. Bellezza, R. T. Hart, and C. F. Burgoyne, "The optic nerve head as a biomechanical structure: Initial finite element modeling," *Invest. Ophthalmol. Visual Sci.* **41**(10), 2991–3000 (2000).
16. M. Asejczyk-Widlicka, D. W. Śródka, H. Kasprzak, and D. R. Is-

kander, "Influence of intraocular pressure on geometrical properties of a linear model of the eyeball: Effect of optical self-adjustment," *Optik (Stuttgart)* **115**(11), 517–524 (2004).
17. H. Kasprzak, "A model of inhomogeneous expansion of the cornea and stability of its focus," *Ophthalmic Physiol. Opt.* **17**, 133–136 (1997).
18. T. N. Wiesel and E. Raviola, "Myopia and eye enlargement after neonatal lid fusion in monkeys," *Nature (London)* **266**, 66–68 (1977).
19. F. Schaeffel, A. Glasser, and H. C. Howland, "Accommodation, refractive error and eye growth in chickens," *Vision Res.* **28**(5), 639–657 (1988).
20. C. Edmund, "Posterior corneal curvature and its influence on corneal dioptric power," *Acta Ophthalmol.* **72**(6), 715–720 (1994).
21. S. Patel, J. Marshall, and F. W. Fitzke III, "Refractive index of the human corneal epithelium and stroma," *J. Refract. Surg.* **11**(2), 100–105 (1995).
22. Z. Liu, A. J. Huang, and S. C. Pflugfelder, "Evaluation of corneal thickness and topography in normal eyes using the Orbscan corneal topography system," *Br. J. Ophthamol.* **83**(7), 774–778 (1999).
23. T. Eysteinsson, F. Jonasson, H. Sasaki, A. Arnarsson, T. Sverrisson, K. Sasaki, E. Stefánsson, and the Reykjavik Eye Study Group "Central corneal thickness, radius of the corneal curvature and intraocular pressure in normal subjects using non-contact techniques: Reykjavik eye study," *Acta Ophthalmol. Scand.* **80**(1), 11–15 (2002).
24. E. Rusinski, *Finite Element Method*, System COSMOS/M, WKL, Wasaw (1994) (in Polish).
25. C. W. McMonnies and G. C. Boneham, "Experimentally increased intraocular pressure using digital forces," *Eye Contact Lens* **33**(3), 124–129 (2007).
26. C. W. McMonnies and G. C. Boneham, "Corneal curvature stability with increased intraocular pressure," *Eye Contact Lens* **33**(3), 130–137 (2007).
27. Y. Le Grand and S. G. El Hage, *Physiological Optics*, Springer Series in Optical Sciences, Vol. **13**, Springer-Verlag, Berlin-Heidelberg-New York (1980).
28. P. M. Kiely, G. Smith, and L. G. Carney, "The mean shape of the human cornea," *Opt. Acta* **29**(8), 1027–1040 (1982).
29. M. Dubbelman, H. A. Weeber, R. G. L. van der Heijde, and H. J. Völker-Dieben,"Radius and asphericity of the posterior corneal surface determined by corrected Scheimpflug photography," *Acta Ophthalmol. Scand.* **80**, 379–383 (2002).
30. M. Baumeister, E. Terzi, Y. Ekici, and T. Kohnen,"Comparison of manual and automated methods to determine horizontal corneal diameter," *J. Cataract Refractive Surg.* **30**(8), 374–380 (2004).
31. W. Lotmar, "Theoretical eye model with aspherics," *J. Opt. Soc. Am.* **61**, 1522–1529 (1971).
32. H. L. Liou and N. A. Brennan, "Anatomically accurate, finite model eye for optical modeling," *J. Opt. Soc. Am. A* **14**(8), 1684–1695 (1997).
33. T. Raphan, "Modeling control of eye orientation in three dimensions. I. Role of muscle pulleys in determining saccadic trajectory," *J. Neurophysiol.* **79**, 2653–2667 (1998).
34. T. Haslwanter, "Mechanics of eye movements: implications of the "orbital revolution," *Ann. N.Y. Acad. Sci.* **956**, 33–41 (2002).
35. J. L. Demer, "Ocular kinematics, vergence, and orbital mechanics," *Strabismus* **11**(1), 49–57 (2003).
36. S. Schutte, S. P. van den Bedem, F. van Keulen, F. C. T. van der Helm, and H. J. Simonsz, "A finite-element analysis model of orbital biomechanics," *Vision Res.* **46**, 1724–1731 (2006).
37. A. Pandolfi and F. Manganiello, "A model for the human cornea: constitutive formulation and numerical analysis," *Biomech. Model. in Mechanobiol.* **5**(4), 237–246 (2006).
38. I. G. Pallikaris, G. D. Kymionis, H. S. Ginis, G. A. Kounis, and M. K. Tsilimbaris, "Ocular rigidity in living human eyes," *Invest. Ophthalmol. Visual Sci.* **46**(2), 409–414 (2005).
39. Y. C. Fung, *Biomechanics: Mechanical Properties of Living Tissues*, Springer-Verlag, NY (1993).
40. B. Jue and D. M. Maurice, "The mechanical properties of the rabbit and human cornea," *J. Biomech.* **19**(10), 847–53 (1986).
41. L. S. Nash, P. R. Greene, and C. S. Foster, "Comparison of mechanical properties of keratoconus and normal corneas," *Exp. Eye Res.* **35**, 413–423 (1982).
42. M. R. Bryant and P. J. McDonnell, "Constitutive laws for biomechanical modelling of refractive surgery," *J. Biomech. Eng.* **118**(4), 473–481 (1996).
43. S. L. Woo, A. S. Kobayashi, C. Lawrence, and, W. A. Schlegel, "Mathematical model of the corneo-scleral shell as applied to intraocular pressure-volume relations and applanation tonometry," *Ann. Biomed. Eng.* **1**(1), 87–98 (1972).
44. J. Liu and C. J. Robert, "Influence of corneal biomechanical properties on intraocular pressure measurement," *J. Cataract Refractive Surg.* **31**, 146–155 (2005).
45. J. L. Battaglioli and R. D. Kamm, "Measurements of the compressive properties of scleral tissue," *Invest. Ophthalmol. Visual Sci.* **25**(1), 59–65 (1984).
46. H. Goldmann and T. Schmidt, "Applanation tonometry," *Ophthalmologica* **134**(4), 221–242 (1957).
47. S. Shah, "Accurate intraocular pressure measurement—the myth of modern ophthalmology?" *Ophthalmology (Philadelphia)* **107**(10), 1805–1807 (2000).
48. R. P. Mills, "If intraocular pressure measurement is only an estimate—then what?" *Ophthalmology (Philadelphia)* **107**(10), 1807–1808 (2000).
49. M. Asejczyk-Widlicka, D. W. Śródka, H. Kasprzak, and B. K. Pierscionek, "Modelling the elastic properties of the anterior eye and their contribution to maintenance of image quality: the role of the limbus," *Eye* **21**(8), 1087–1094 (2007).
50. J. S. Friedenwald, "Contribution to the theory and practice of tonometry," *Am. J. Ophthalmol.* **20**, 985–1024 (1937).